POUROUS LIQUID METAL-ELASTOMER COMPOSITES

A Thesis

presented to

the Faculty of the Graduate School

at the University of Missouri-Columbia

In Partial Fulfillment

of the Requirements for the Degree

Master of Science Mechanical Engineering

---

by

BRIAN ARENDS

Dr. Zheng Yan, Thesis Supervisor

MAY 2023

The undersigned, appointed by the dean of the Graduate School, have examined the thesis entitled
POUROUS LIQUID METAL-ELASTOMER COMPOSITES

presented by Brian Arends,

a candidate for the degree of Master of Science, and hereby certify that, in their opinion,

it is worthy of acceptance.

_____

Professor Zheng Yan

_____

Professor Jian Lin

_____

Professor Ilker Ozden

ACKNOWLEDGEMENTS

I would like to express my heartfelt gratitude to all those who have supported and contributed to the completion of this engineering thesis. First and foremost, I extend my deepest appreciation to my supervisor Dr. Zheng Yan for accepting me into their lab for this research process. Their expertise and dedication have been instrumental in shaping the direction of this thesis. I would also like to thank Yadong Xu and our research team for their collaborative efforts, stimulating discussions, and technical assistance. Lastly, I would like to acknowledge the funding from the University of Missouri-Columbia and other agencies that have provided financial support for this research. Their support has been crucial in realizing the goals of this thesis.

TABLE OF CONTENTS

LIST OF ILLUSTRATIONS

Figure Page

LIST OF TABLES

Table Page

ABSTRACT

It is known that liquid metal–elastomer composites are promising soft conductors for skin-interfaced bioelectronics, soft robots, and other applications due to their large stretchability, ultrasoftness, high electrical conductivity, and mechanical-electrical decoupling. There is, however, a high level of deformation-induced leakage, which can result in smears on the skin, poor performance of the device, and short circuits in the circuit. By using phase separation, we describe the synthesis of porous liquid metal–elastomer composites with high leakage resistance and antimicrobial properties.

Furthermore, these composites exhibit high stretchability, tissue-like compliance, high electrical conductivity, high breathability, and compatibility with magnetic resonance imaging. As a result of damping effects, porous structures can minimize leakage and reduce liquid metal usage. In addition to monitoring cardiac electrical and mechanical activity, skin-interfaced bioelectronics can deliver electrical stimulation in a mechanically imperceptible and electrically stable manner.

1 INTRODUCTION

In recent years, there has been significant advancement in the field of next-generation skin-interfaced bioelectronics, specifically in the development of elastic soft conductive materials that possess tissue-like compliance and high stretchability. These materials are crucial for establishing intimate and prolonged contact with soft biological tissues, while maintaining stable and reliable electronic functionality even under dynamic deformations. These advancements can be primarily attributed to two main approaches: (i) employing structural designs such as serpentine, wavy, island-bridge, and kirigami to enable stretchability in non-stretchable inorganic materials, and (ii) creating intrinsically stretchable materials, such as organic conductors, elastomer composites, and hydrogels [1-8].

Although the methods mentioned above provide significant flexibility in creating stretchable conductive materials, they typically encounter certain limitations. For instance, structural designs do not address the microscopic rigidity of inorganic materials, resulting in a noticeable mismatch in elastic moduli between these materials and the soft biological tissues they interface with. Organic conductors, on the other hand, often exhibit relatively high elastic moduli and low electrical conductivity. Furthermore, hydrogels pose challenges related to their poor electrical conductivity and limited long-term stability due to dehydration.

One promising strategy among these approaches is the incorporation of conductive fillers into elastomers, which combines the high electrical conductivity of the fillers with the superelasticity, stretchability, and tissue-like compliance of elastomers

[9-11]. In comparison to rigid inorganic fillers like silver nanowires (AgNWs) and silver flakes, liquid metal, particularly eutectic gallium-indium (EGaIn) nano/microparticles consisting of EGaIn cores and gallium oxide shells (Ga2O3; ~3 nm thick), has gained increasing interest due to its excellent metallic electrical conductivity (~3.4 × 106 S/m), liquid-like fluidity, negligible vapor pressure (~10−44 atm), and non-toxicity [12]. Recently, elastomer composites embedded with EGaIn have been developed, demonstrating large stretchability, high electrical conductivity, and minimal conductance variations upon deformation [13-15]. Furthermore, breathable EGaIn-elastomer composites have been achieved by directly coating bulk EGaIn on fibrous mat surfaces [16]. However, one limitation of liquid metal-embedded elastomer composites is the issue of undesired leaking during deformations, which can result in skin smearing, device performance degradation, and electrical shorting [15]. For example, the resistance of liquid metal fiber mat can increase by ~50% when rubbed against human skin [16]. While encapsulation can minimize leakage and improve durability, it can also complicate the fabrication process and hinder direct interface with human skin in applications such as cutaneous bioelectronic sensing and stimulation.

In this study, we present a phase separation-based synthesis method for creating EGaIn-embedded porous, soft conductors that are also incorporated with epsilon polylysine (ε-PL). This approach offers several significant advancements, including: (i) achieving high leakage resistance under various deformations in liquid metal-embedded soft conductors; (ii) reducing the usage of liquid metal in elastomer composites due to significantly reduced percolation thresholds.

Furthermore, the porous, soft conductor obtained from this synthesis method exhibits remarkable properties, such as large stretchability, tissue-like compliance, high and stable electrical conductance over deformation, high breathability, and compatibility with magnetic resonance imaging (MRI). The unique combination of these attributes is critical for enabling long-term, stable, and sustainable operation of soft bioelectronics on the skin in versatile daily life scenarios.

Moreover, we demonstrate the application of these porous, soft conductors in skin-interfaced bioelectronics and interconnection cables. These devices can concurrently monitor cardiac electrical activities (electrocardiograms or ECGs) and mechanical activities (impedance cardiograms or ICGs), offer programmed electrical stimulations, and operate stably and reliably even under dynamic deformations. Importantly, these devices are mechanically imperceptible to users, enhancing their comfort and usability in practical applications [41].

2 PROBLEM STATEMENT & THESIS CONTRIBUTIONS

The main goal of this thesis is the design of a Liquid metal–elastomer composite that has the desired properties for an on skin bioelectronic device. The aims of this thesis are:

(1)Create a soft conductor for skin-interfaced bioelectronics, soft robots and,

(2) To analyze its stretchability, ultrasoftness, high electrical conductivity, and mechanical-electrical decoupling.

Achieving these goals involved the following three tasks:

1. Fabricating the material from previous works,
2. Improving on the process to create new material properties for the desired outcome,
3. Analysis of the material results.

3 PROCESSES

3.1 Material Fabrication

In this study, we propose a novel approach for synthesizing EGaIn-embedded porous, soft conductors with epsilon polylysine (ε-PL) using phase separation, in contrast to conventional methods that involve mixing liquid metal particles with elastomers. Here in Figure 3.1 PU is used as elastomer matrices. In our approach, porous structures are created during phase separation, which offer damping effects to minimize leakage caused by mechanical deformation shown in Figure 3.2. Additionally, ε-PL, a safe and natural antimicrobial peptide, is loaded into the elastomer matrices during phase separation to

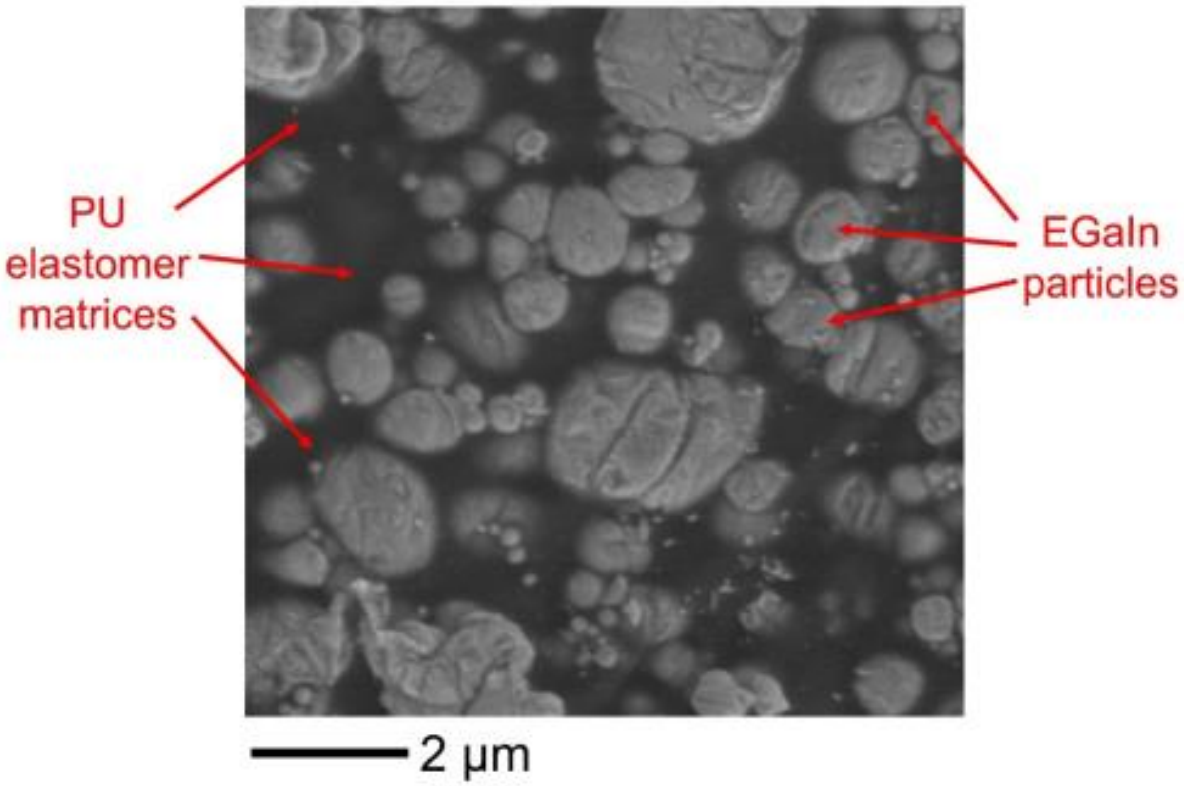

Figure 3.1: SEM image of nonporous EGaIn composites before mechanical sintering.

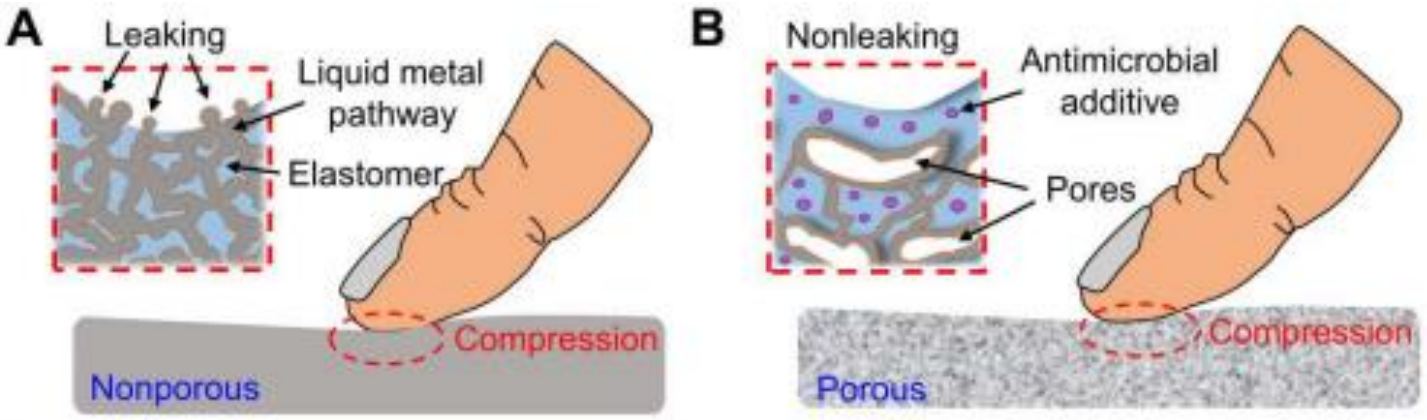

Figure 3.2: Multifunctional nonporous (**A**) and porous (**B**) EGaIn composites upon compression.

impart antibacterial and antiviral properties. EGaIn particles and polyurethane (PU) are used as conductive fillers and elastomer matrices, respectively.

The fabrication process seen in figure 3.3 involves tip sonication of EGaIn in 1-butanol to break the bulk liquid metal into micro/nano-sized particles, followed by addition of the BEHS-modified ε-PL and PU solution in tetrahydrofuran (THF). The resulting precursor solution is dropcasted on an aluminum foil and dried in air. The rapid evaporation of THF triggers phase separation of 1-butanol to form nano/microscale droplets (i.e., PU poor phase). Subsequent complete evaporation of THF and 1-butanol leads to the formation of porous EGaIn composites. During phase separation, EGaIn particles self-organize on pore surfaces due to the Pickering effect, resulting in the formation of conductive pathways by mechanical sintering. Finally, laser cutting is used to define arbitrary patterns on the obtained porous EGaIn composites for device fabrication.

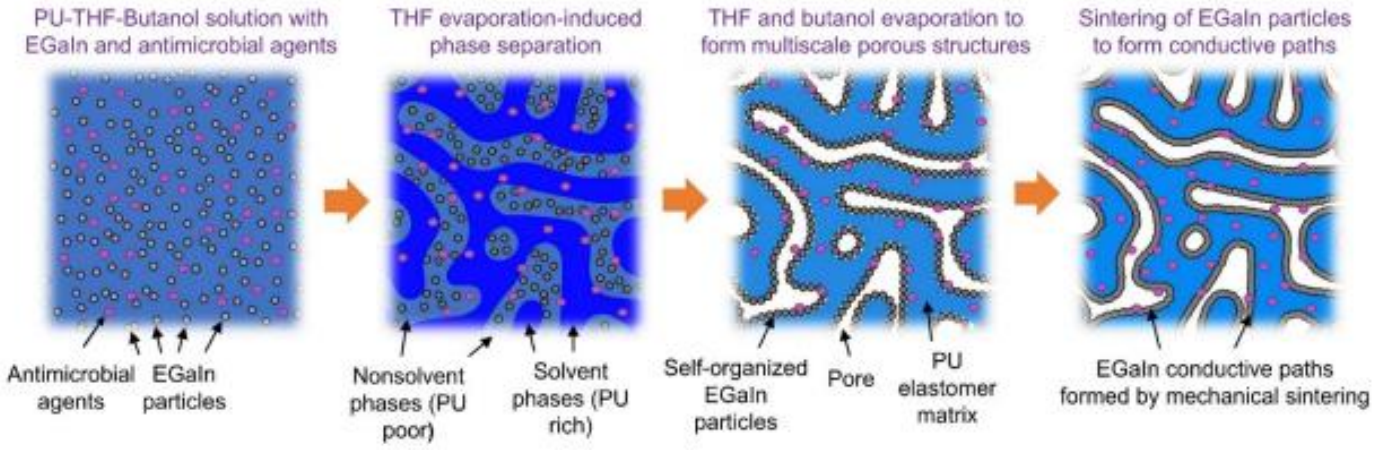

Figure 3.3: Schematic of phase-separation-based synthesis of multifunctional porous EGaIn composites

The electrical conductivity of the porous EGaIn composite can be tailored by adjusting the EGaIn volume fraction, with a maximum value of ~1.2 × 106 S/m achieved at ~55% EGaIn volume fraction. In this work, we used 25% EGaIn volume fraction for characterization and device fabrication, striking a trade-off between device performance and EGaIn usage. The resulting porous EGaIn composites exhibit a porosity of ~57% and an electrical conductivity of ~2.0 × 105 S/m.

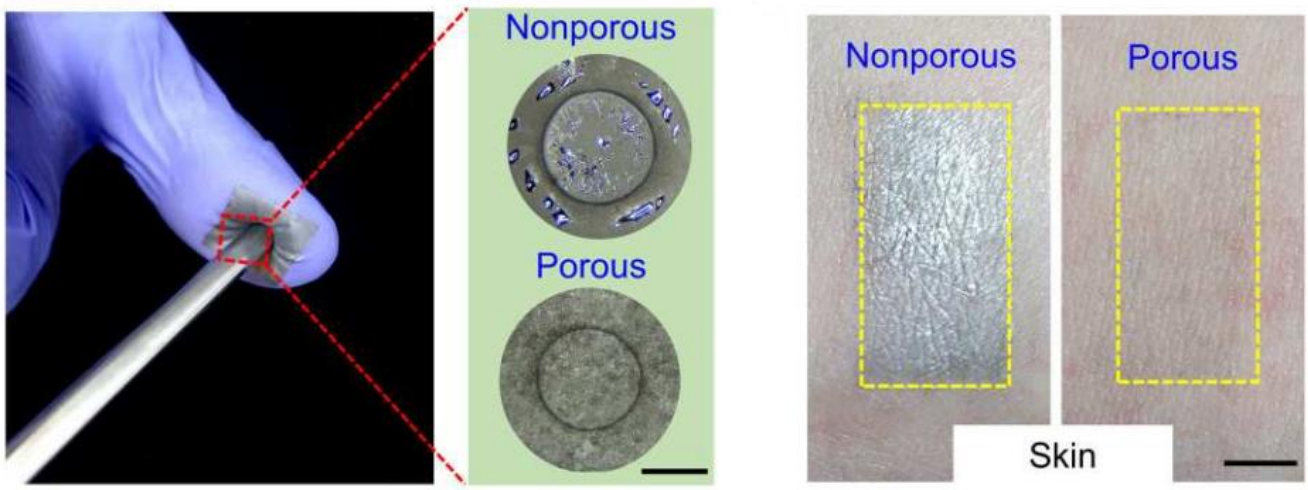

Figure 3.4: Photographs of compressing EGaIn composites with a stainless-steel 584 rod and human skin after wearing nonporous versus porous EGaIn composites for three days

3.2 Finite Element Analysis

Compared to conventional nonporous liquid-metal composites, the conductive pathways of porous EGaIn composites are located at the interfaces between the solid elastomer and gas-filled pores, resulting in significantly lower stress during mechanical loading due to the damping effects of the porous structures. This outstanding leakage resistance under deformation is demonstrated in Figure 3.4 and is supported by finite

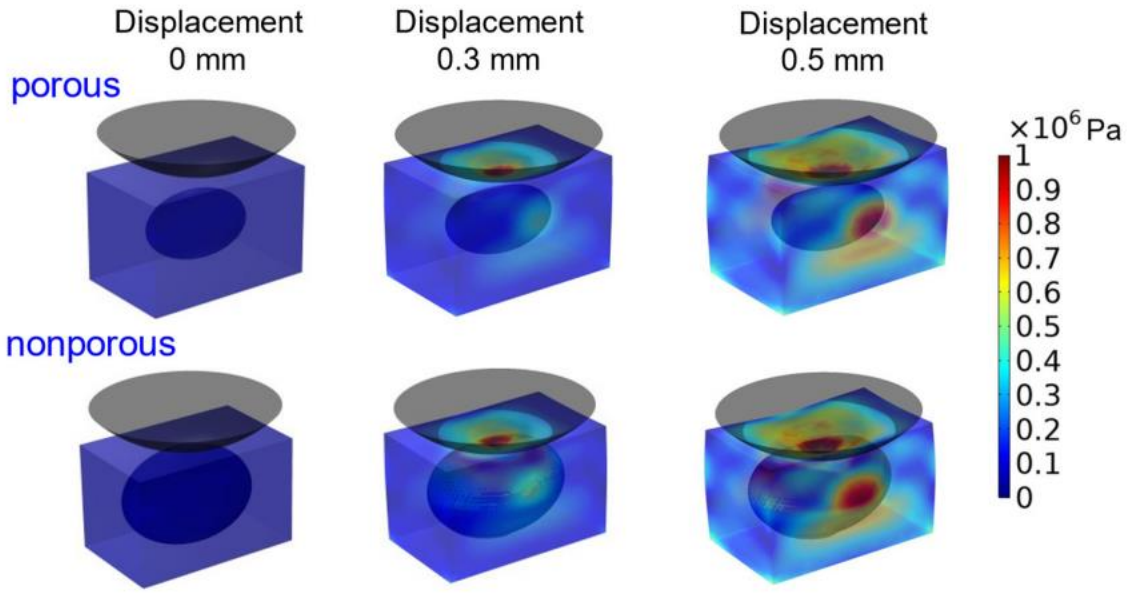

Figure 3.5: FEA simulations of nonporous and porous EGaIn composites upon mechanical compression

element analysis (FEA) simulations (Figures 3.5 and S2). The ratio of average stress on EGaIn pathways in nonporous and porous composites as a function of applied displacement. The findings demonstrate a significant reduction in average stresses on EGaIn pathways in porous composites, attributed to the damping effects of porous structures. To theoretically study the leakage resistance of EGaIn composites under mechanical loading, finite element analysis (FEA) simulations were performed using the solid-mechanics model in COMSOL-Multiphysics, with a stationary analysis. A 3D model was adopted for the simulation, with a sandwich structure featuring EGaIn pathways sandwiched between the polyurethane (PU) matrix and air, for the porous composites, and the PU matrix for nonporous composites. The simulation dimensions comprised an 8 x 5 x 5 mm PU rectangular block and a 3.2 x 2.2 x 2.2 mm ellipsoidal EGaIn path. Compression was applied using a rigid circular shell with contact boundary

conditions. The results showed that the average stress on the EGaIn path decreased considerably in porous composites compared to nonporous composites when subjected to compressive loads, as depicted by the distributions of von Mises stresses in porous and nonporous EGaIn composites under finger-like compressions. These findings contribute to a better understanding of the mechanical behavior of EGaIn composites under compressive loads, highlighting the importance of porous structures in reducing stresses on EGaIn pathways.

3.3 Devices

Nonporous and porous EGaIn composites with similar electrical conductivity (~2.0 × 105 S/m) were compared for their leakage resistance. Compression on nonporous composites resulted in evident EGaIn leakage, while porous composites showed negligible leakage (Figure 3.4, right panel) even after wearing for 3 days, as opposed to visible smearing observed on human skin with nonporous composites (Figure 3.4, left panel). Moreover, repetitive compression (0.4 MPa for 100 cycles) caused circuit shorting of adjacent conductive traces in nonporous composites (Figure S3 and S4), while porous composites showed negligible effects on adjacent traces. Similarly, cyclic stretching (400% strain for 100 cycles) induced severe leakage on nonporous composites, whereas negligible leakage was observed on porous composites. The estimated leakage from nonporous composites in Figure S3 was ~0.22 g/cm3 at 400% strain. The threshold for EGaIn leakage in porous composites was experimentally determined to be ~0.9 MPa

Figure 3.6: Photographs of light-emitting diode arrays, interconnected with conductive traces of porous EGaIn composites

under compression, and no leakage was observed until the porous composite ruptured at ~550% strain. Furthermore, collapsing of the porous structures via dimethylformamide vapor treatment caused EGaIn leakage from the collapsed composite upon stretching (figure S8), highlighting the critical role of porous structures in achieving high leakage resistance. Additionally, Figure 3.5 demonstrates that the "SMBE" light-emitting diode array, interconnected with conductive traces of porous EGaIn composites patterned on porous polyurethane, can operate stably and reliably even under large stretching (200% strain).

Skin-interfaced bioelectronic systems consisting of skin-mounted bioelectronic patches with porous EGaIn composite electrodes on porous polyurethane (PU) substrates, imperceptible cables of porous EGaIn composites, and mobile data acquisition modules. The system includes rigid data acquisition modules clipped onto clothing to avoid direct contact with the skin, which are connected to skin-mounted bioelectronic patches with superelastic, ultrasoft cables of porous EGaIn composites. The resulting wearable system is mechanically imperceptible, comfortable for users, and capable of high-fidelity signal

recording even during human motions and in water. The skin-mounted bioelectronic patches and interconnection cables, based on solution-processed porous composites, are disposable to minimize infection risks, and the clothing-clipped data acquisition modules can be easily dismantled from the wearable systems for reuse to save cost. This form of wearable device represents a valuable addition to existing wearable systems integrated on a single substrate and provides a low-cost and one-time use solution to the recording of high-fidelity signals.

We investigated the fundamental aspects of mechanical imperception in skin-mounted electronic patches. It is known that the skin sensation limit is approximately 20 kPa, and most mechanoreceptors that sense stimuli are located in the dermis. To evaluate the stress on the skin surface and bottom epidermal layer caused by stretching cables connected to skin-mounted electronic patches, we performed numerical simulations using finite element analysis (FEA). The FEA simulations (Fig. 3.7) revealed the stresses caused by stretching the widely used flexible anisotropic conductive film (ACF) cable and the porous EGaIn composite cable. To induce the 20-kPa stress on the skin surface, a strain of ~0.2 and 46% (a factor of ~230) are required for stretching ACF cables and porous EGaIn composite cables, respectively. The simulation and experimental results indicate that the porous EGaIn composite cables are highly imperceptible compared to ACF cables. These findings demonstrate the potential of porous EGaIn composite cables for use in skin-mounted electronic patches that require high mechanical imperceptibility. Questionnaires were employed to assess the discomfort levels of skin-interfaced bioelectronic systems as shown in figure 3.8. The wearable systems consisted of skin-mounted bioelectronic patches connected to clothing-clipped mobile data acquisition

modules via different types of cables, including porous composite cables, ACF cables, and conventional PVC-insulated copper wires. To evaluate the comfort levels of the wearable systems, twenty participants were recruited, and their discomfort levels were assessed using visual analog scales ranging from 0 to 10 after wearing the systems for 24 hours. The results showed that the wearable systems interconnected with porous EGaIn composite cables exhibited significantly lower discomfort levels as compared to those interconnected with ACF cables and PVC-insulated copper wires. This superior comfort can be attributed to the ultrastretchability and ultrasoftness of porous EGaIn composite cables.

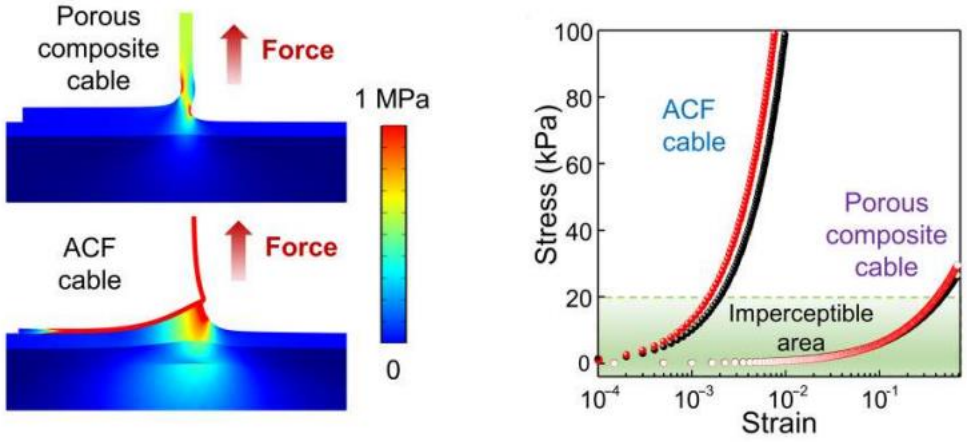

Figure 3.7: Simulation results for the von Mises stress distribution when stretching (left) and Simulation results for stresses induced on the skin surface (red) and the bottom epidermis (80 μm in depth; black) as a function of strains applied to the porous EGaIn composite cable and the ACF cable (right)

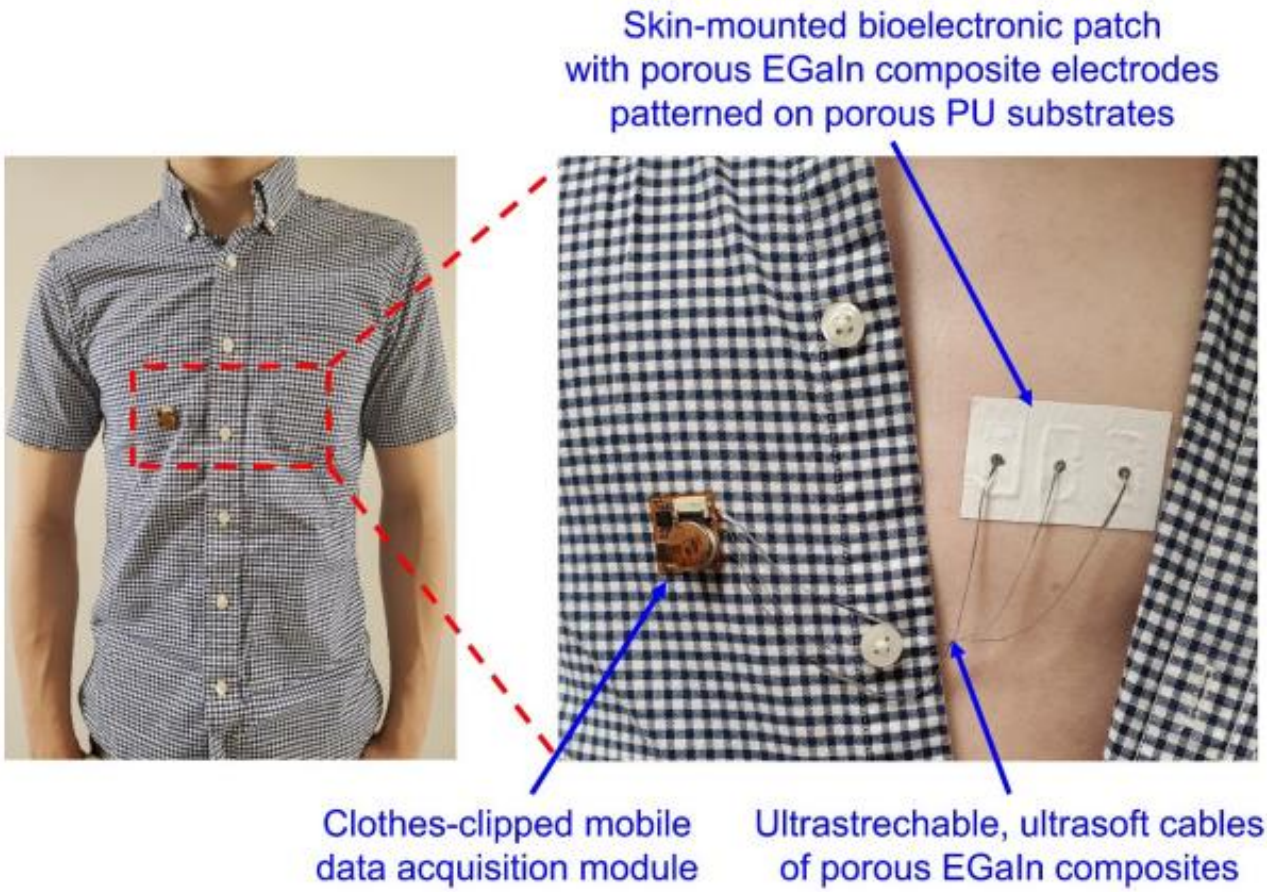

Figure 3.8: Photographs of the skin-interfaced bioelectronic system based on porous EGaIn composites

3.4 ECG and ICG

Ascertaining heart electrical activity through ECG, outside of clinical settings, is a critical aspect of diagnosing heart diseases. Simultaneously monitoring cardiac mechanical function through ICG provides complementary and valuable information to ECG [42-44]. In this regard, the wearable system utilizing porous EGaIn composites records high-fidelity ECG and ICG even during human motions. Additionally, the porous

EGaIn composite electrodes demonstrate comparable skin-electrode impedance (~70 kilohms) to that of Ag/AgCl gel electrodes (~65 kilohms) of the same dimension (10 mm × 20 mm) at 100 Hz. Concurrent ECG and ICG signals are shown in figure S6 respectively, as illustrated in figure S7. The ECG signals depict distinguishable p-wave, QRS complex, and t-wave, while ICG critical characteristic points such as B, C, X, and O (representing the opening of the aortic valve, maximum ejection velocity, closing of the aortic valve, and opening of the mitral valve, respectively) are clearly observable [42]. Furthermore, the pre-ejection period (i.e., time elapse between the Q point in ECG and B point in ICG) represents the period of left ventricular contraction with cardiac valves closed and is indicative of heart sympathetic innervation [44].

The mechanical properties of the porous EGaIn composite enable steady biosignal recording with high signal-to-noise ratios (SNRs) under dynamic deformations, making it an ideal candidate for skin-interfaced electrodes and interconnection cables (Fig. S8, and figs. 3.9 and 3.10). Compared to conventional Ag/AgCl gel electrodes and other soft conductors such as Ag flake–PU composites and AgNW-PU composites, these electrodes and cables demonstrate superior stretchability, ultrasoftness, and stable conductance over strain. The reliability and stability of signal acquisitions are demonstrated even during motions, as shown by concurrent ECG and ICG signal recording during stationary bike riding and ECG monitoring during rest, walking, and jogging on a treadmill (fig. 3.11). Porous EGaIn composite electrodes can also deliver reliable, programmed electrical stimulations even under deformations (fig. S9). With the high hydrophobicity of porous PU (water contact angle, 140°), the skin-interfaced bioelectronics made with these

materials demonstrate excellent waterproofness and can perform high-quality electromyogram (EMG) recording even in water.

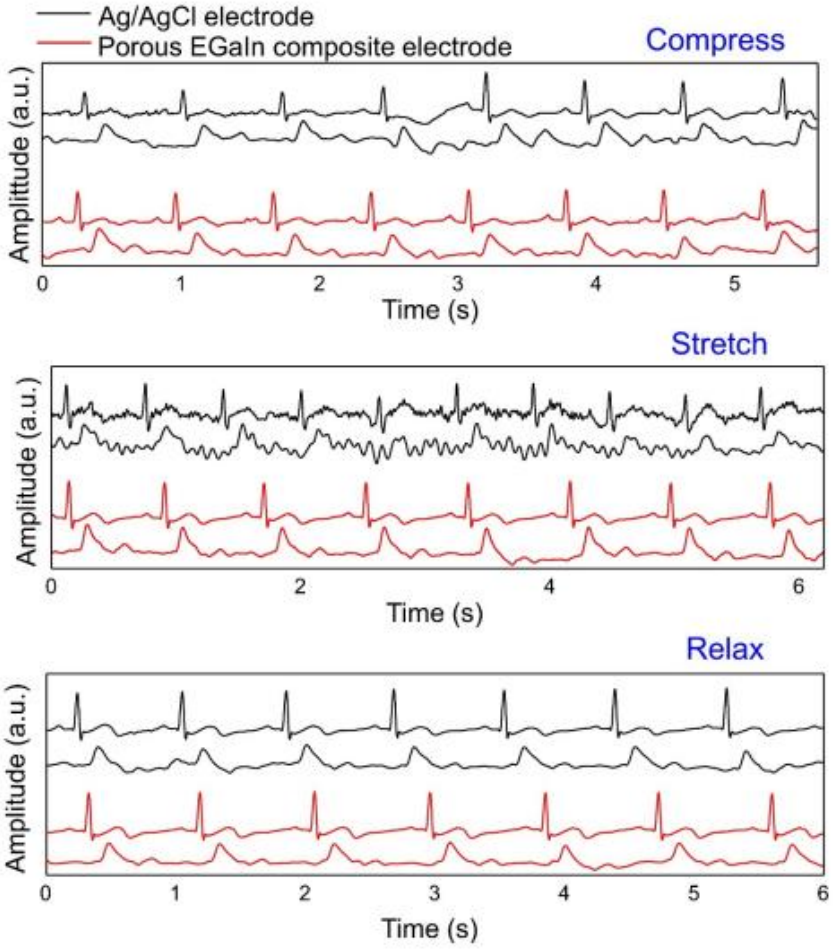

Figure 3.9: ECG and ICG signals recorded by Ag/AgCl electrodes (black) and porous EGaIn composite electrodes (red) when compressing, stretching, and relaxing these electrodes

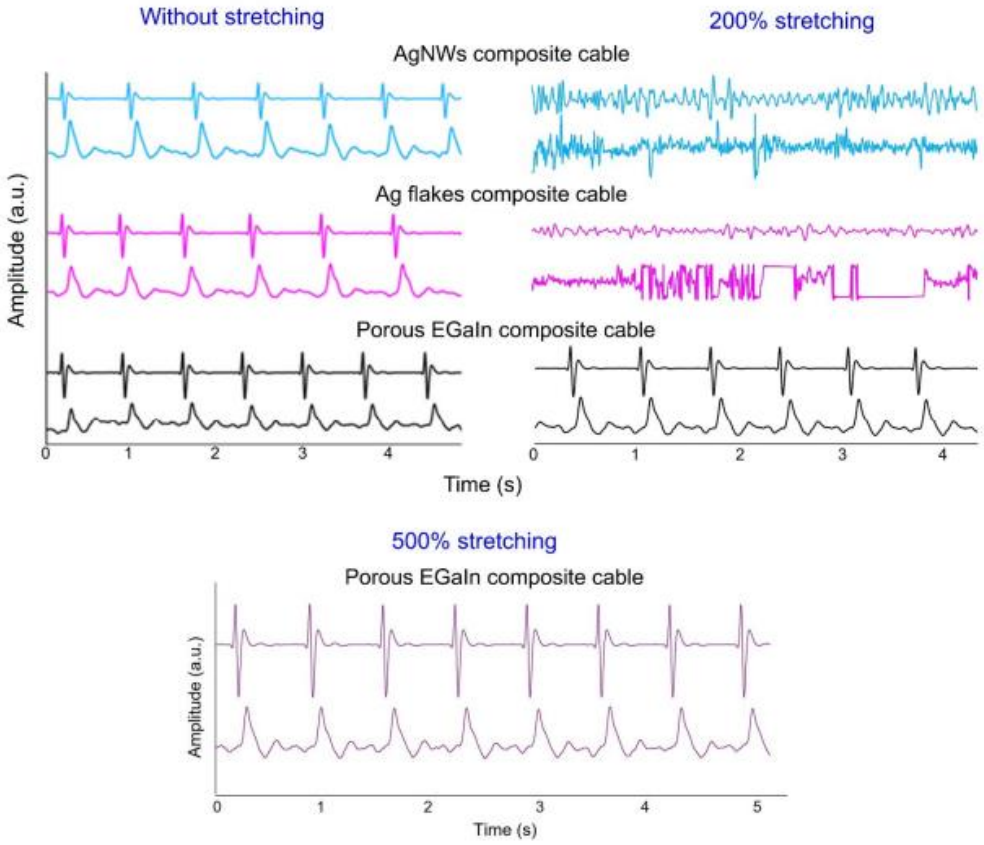

Figure 3.10: ECG and ICG signals recorded using porous EGaIn composite electrodes when stretching various cables with 0%, 200% and 500% strains

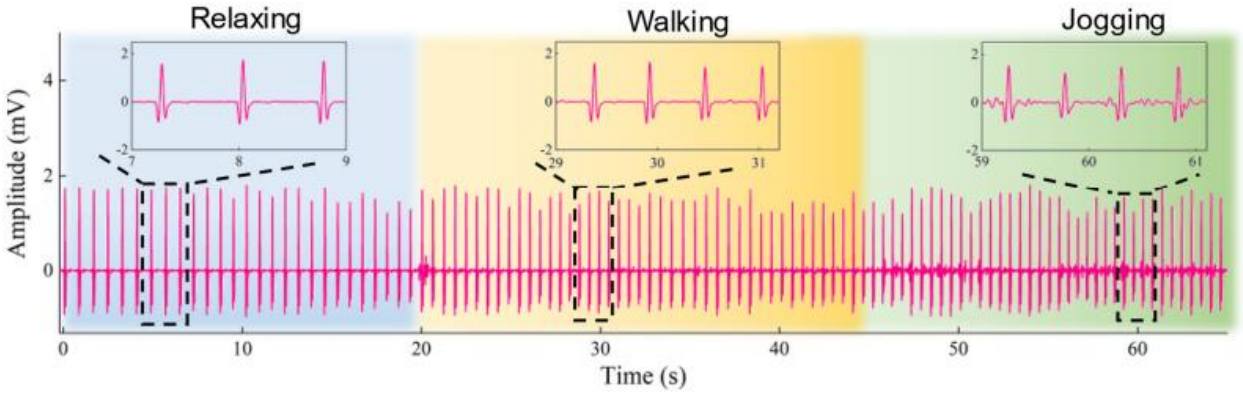

Figure 3.11: ECG signals recorded using the wearable system, shown in fig. S25, when human subject relaxed (blue), walked (orange) and jogged (green) on a treadmill

4 RESULTS

The size of EGaIn particles can be controlled by adjusting the sonication time, as shown in Figure 4.1. Smaller particle sizes result in lower electrical conductivities of the porous EGaIn composites at the same volume fraction (~25% in this study), possibly due to increased amounts of oxide skin layers such as Ga2O3. For the preparation of EGaIn composites in this work, EGaIn particles with a diameter of approximately 1.26 μm were obtained using 2-min sonication.

Compared to nonporous EGaIn composites, porous composites with phase separation-induced structures show significantly lower percolation thresholds. Percolation threshold is the critical point at which the electrical conductivity experiences a sharp transition as the number of conductive fillers increases. As shown in Figure 4.2, the percolation threshold of the porous composite (~0.07) is considerably lower than that of the nonporous composite (~0.39), due to the self-assembly of EGaIn micro/nanoparticles on the pore surfaces instead of uniform distributions in elastomer matrices.

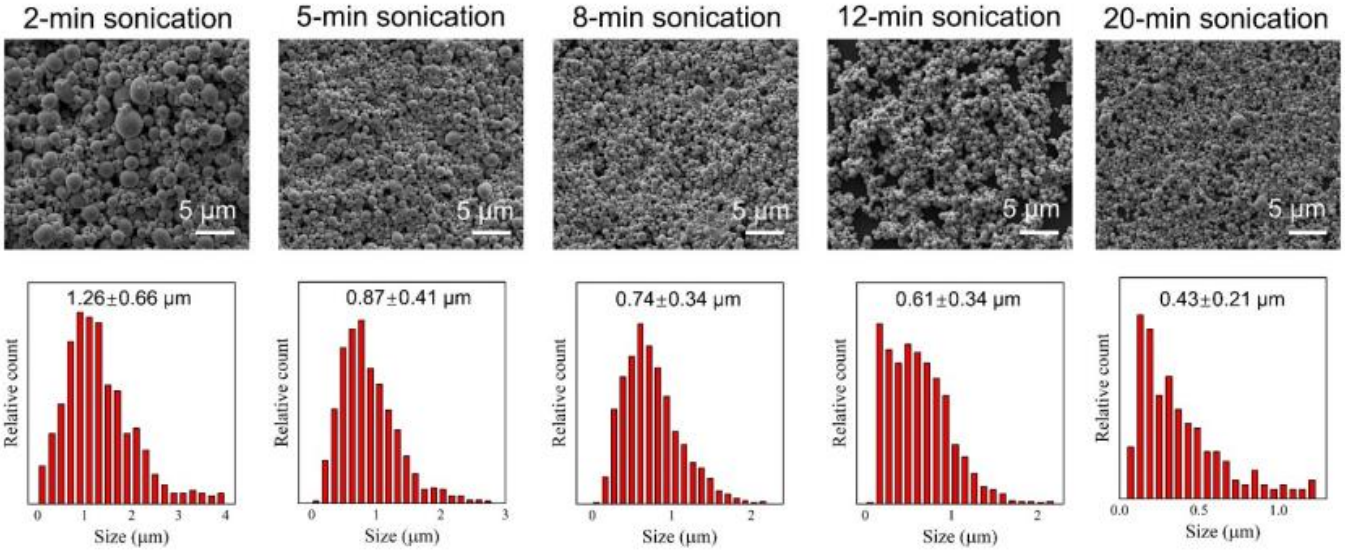

Figure 4.1: Preparation of EGaIn particles by tip sonication

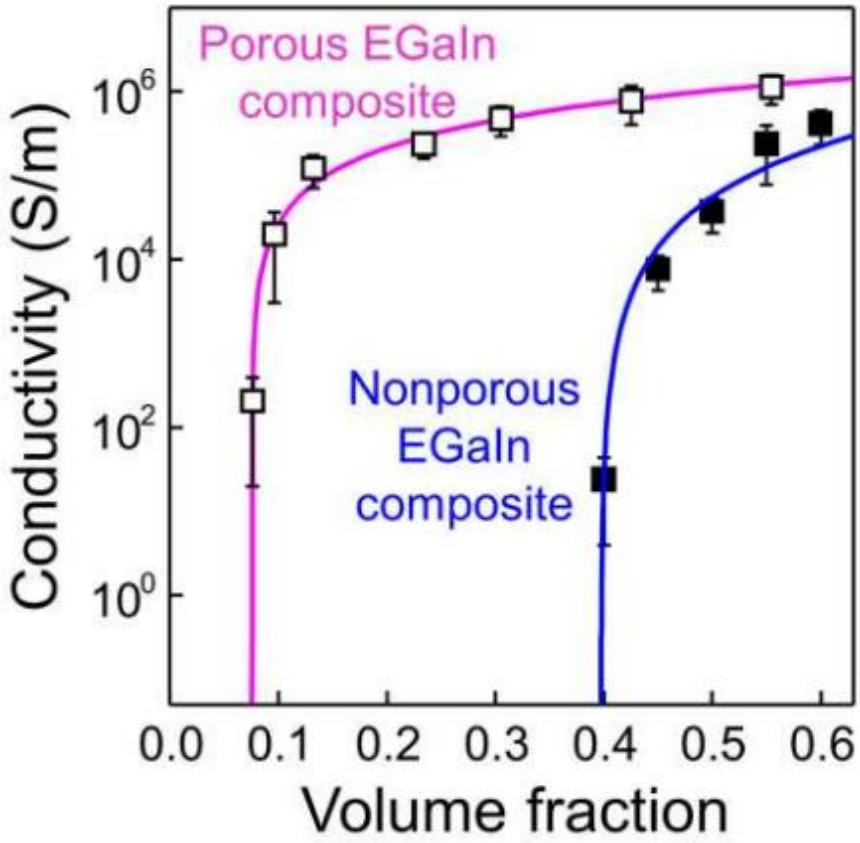

Figure 4.2: Electrical conductivities of nonporous and porous EGaIn composites as a function of EGaIn volume fractions

This reduced percolation threshold means that less EGaIn is required in the porous composite compared to the nonporous composite to achieve the same electrical conductance. For instance, the usage of EGaIn in porous composites is only about 33% of that in nonporous composites to achieve an electrical conductivity of ~2.0 × 105 S/m, which is sufficient for applications in soft bioelectronic electrodes and conductive interconnects. Furthermore, a high electrical conductivity of ~1.2 × 106 S/m can be achieved when the volume fraction of EGaIn in the porous composite is approximately

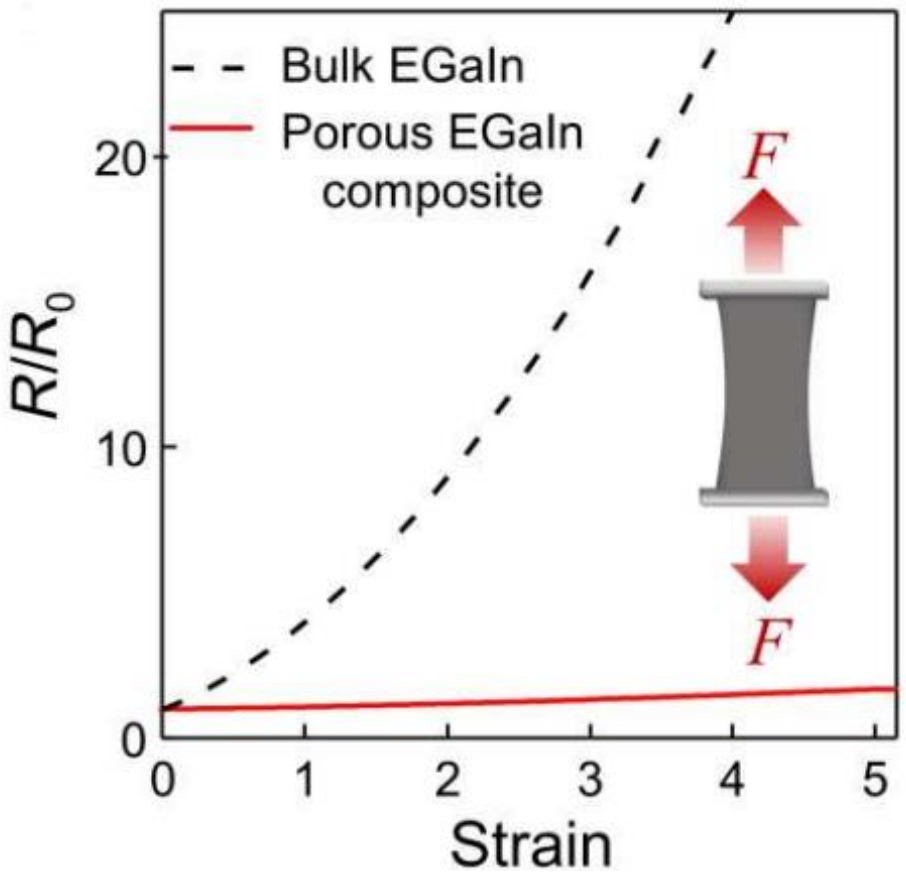

Figure 4.3: Relative resistance changes (R/R0) of bulk EGaIn and porous EGaIn composites as a function of uniaxial strains.

55%. Notably, the obtained porous EGaIn composites exhibit exceptional electrical uniformity over a large area. Soft conductors ideally should exhibit stable conductance even under various deformations, maintaining mechanical-electrical decoupling. This characteristic is crucial for the construction of bioelectronics and soft robots that need to function reliably under dynamic motions. Remarkably, as shown in Figure 4.3 and Figure S5, the porous EGaIn composites demonstrate minimal change in conductance upon both

uniaxial and biaxial stretching, which is substantially lower than that predicted by Pouillet's law for bulk EGaIn [25]. This unique behavior arises from fluid-like nature

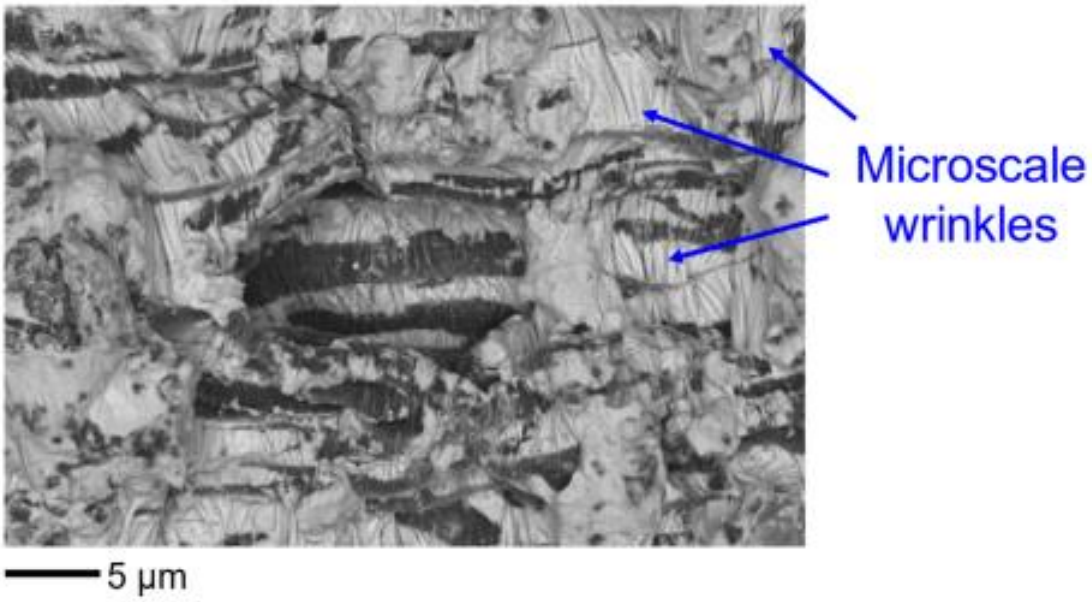

Figure 4.4: High-resolution SEM image of porous EGaIn composites

of liquid metal, reorientation of tortuous conductive pathways during stretching, and the formation of microwrinkles due to the mechanical mismatch between the liquid core and the solid shell, as illustrated in Figure 4.4.

Furthermore, the electromechanical responses of the porous EGaIn composites are relatively unaffected by the EGaIn fraction and stretching rate, as shown in Figure 4.5. Notably, the porous composites exhibit outstanding durability and reliability, with only ~15% change in resistance after cyclic stretching of 500% for 1000 cycles, as depicted in Figure 4.6. In comparison to recently developed breathable liquid metal fiber mats [16], the porous EGaIn composites show minimal resistance changes (~20%) even after repetitive peeling using scotch tapes for 100 cycles, as demonstrated in Figure 4.7. This

exceptional electrical property is further corroborated by stable and robust electrocardiogram (ECG) recording after up to 100 peeling cycles. Additionally, the porous composites also exhibit high electrical stability under various conditions, including ambient conditions, phosphate-buffered saline (PBS) solutions, ultraviolet ozone treatment, and repetitive washing.

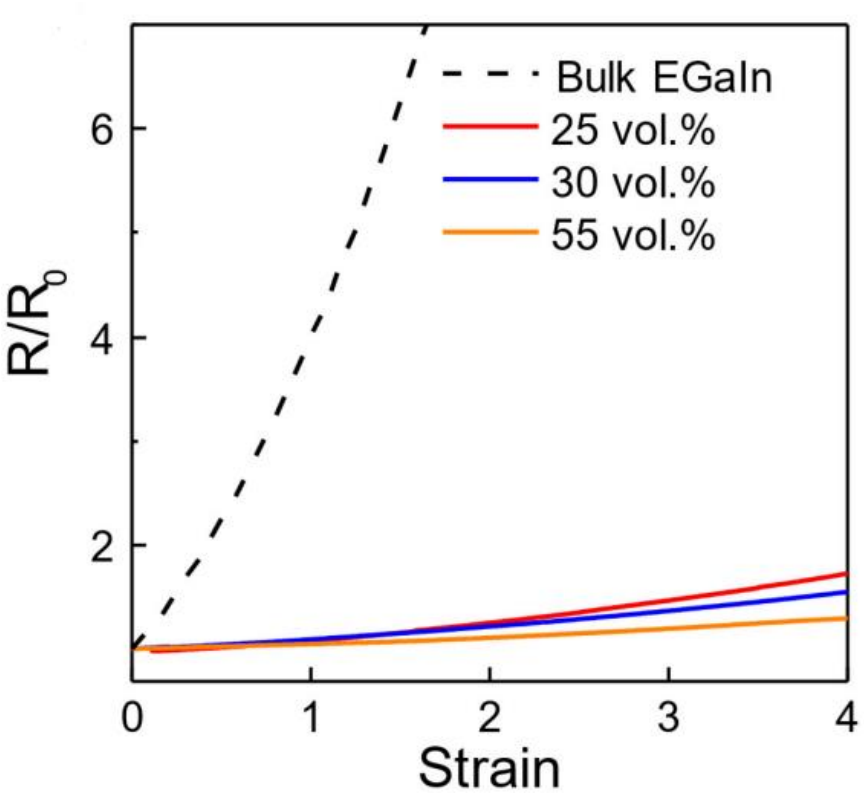

Figure 4.5: Effects of EGaIn contents on electrochemical responses of porous EGaIn composites

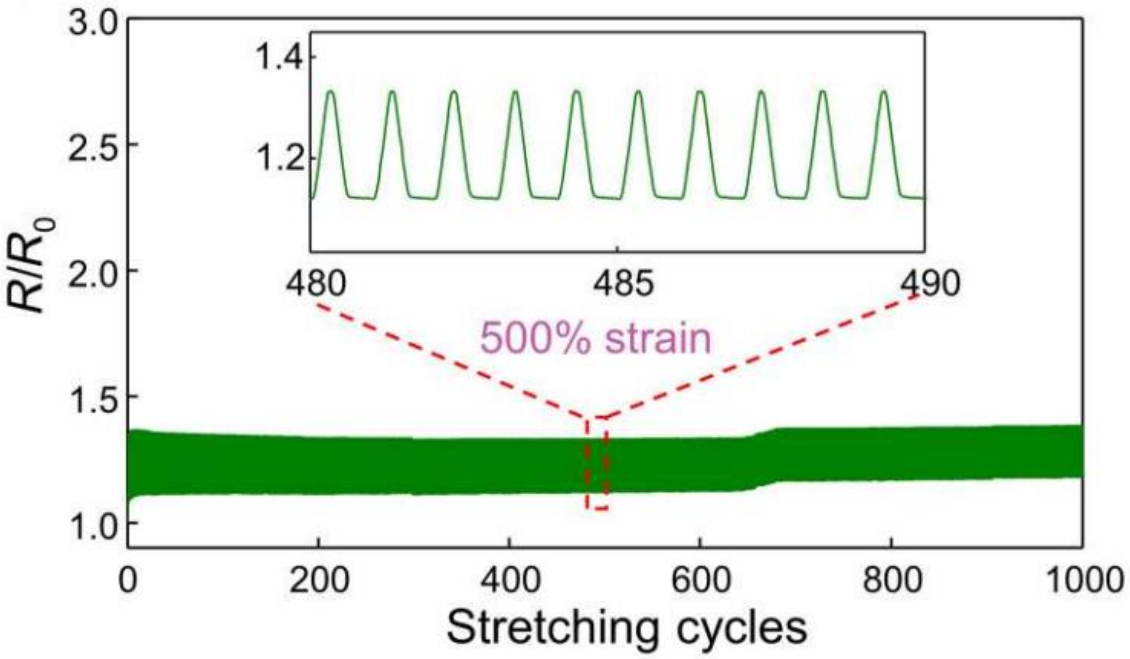

Figure 4.6: Relative resistance changes of porous EGaIn composites subjected to cyclic stretching

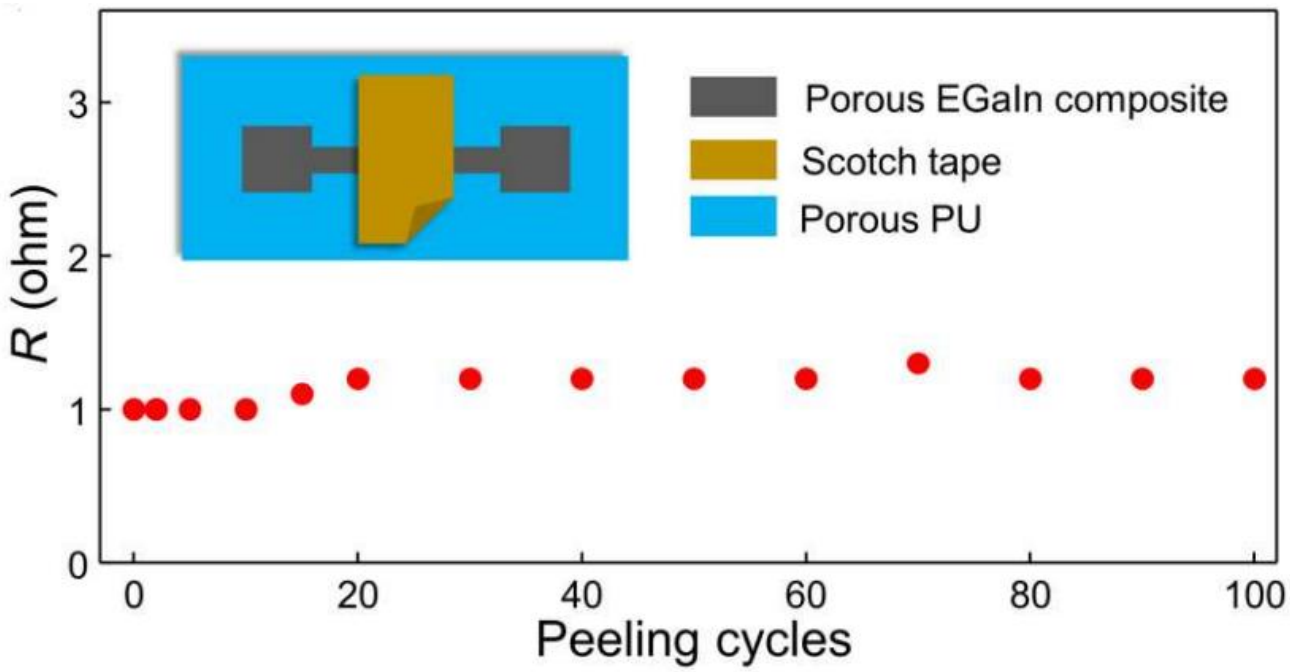

Figure 4.7: Resistance changes of porous EGaIn composites under cyclic peeling with scotch tapes

Moreover, due to the supercooling effect of liquid metal [26] and the high human body temperature, the porous EGaIn composites remain soft and functional even in extreme winter scenarios. This highlights the excellent performance and versatility of the porous EGaIn composites as soft conductors for diverse applications.

Breathability is a crucial requirement for skin-interfaced bioelectronics, as it facilitates skin perspiration and enhances long-term biocompatibility [27]. The interconnected pores in the porous EGaIn composite enable high breathability. The water vapor transmission rate of the porous composite (~4900 g m−2 day−1) is comparable to that of an open bottle (~6800 g m−2 day−1), and notably higher than those of nonporous EGaIn composites (~340 g m−2 day−1) and human skin (~200 g m−2 day−1) [31]. It is known that the elastic modulus (E) of a material scale with its density (ρ) following the

equation $E/Es \propto (\rho/\rho s)\, n$ [29], where the power (n) depends on the nano/microstructures of the porous material. The elastic modulus of the porous EGaIn composite is remarkably low, measuring around ~1.5 MPa, which is approximately 10 times lower than that of nonporous composites (~16.7 MPa), and comparable to the elastic modulus of human skin (~5 kPa to 140 MPa) [30].

Table 4.1: Material properties used for simulations

Material	Youngs Modulus	Poisson's Ratio
Porous Composite	1.5 MPa	0.2
PU	15 MPa	0.4
ACF Cable	3 GPa	0.34
EGaIn	Bulk modulus 50 MPa (53) Shear modulus 1 kPa (53)	Not Used
Epidermis	2.5 MPa (54)	0.4
Dermis	10 MPa (55)	0.4

5 DISCUSSIONS

Using a carefully designed phase separation approach, we have successfully developed multifunctional porous, soft conductors based on EGaIn, featuring high leakage resistance and antimicrobial properties, along with other desirable characteristics such as large stretchability, tissue-like compliance, stable electrical conductance during deformation, high breathability, and MRI compatibility. During the phase separation process, EGaIn particles self-organize on the surfaces of the pores and form conductive pathways through mechanical sintering. This not only lowers the percolation thresholds and reduces the amount of EGaIn used (requiring only ~33% of EGaIn compared to nonporous composites with the same electrical conductivity at ~2 × 105 S/m), but also minimizes leakage of liquid metal caused by deformation.

The incorporation of ε-PL through phase separation enables the obtained porous, soft conductor to exhibit remarkable antibacterial and antiviral properties remarked by another member in this lab. These unique features make it an ideal soft conductor with built-in multifunctionality for constructing skin-mounted bioelectronic patches and interconnection cables for long-term, home-based biomedical applications. The resulting wearable device can seamlessly interact with the human body, providing comfortable and imperceptible mechanical sensation, while delivering high-fidelity and stable biosignal recording, as well as programmed bioelectronic interventions, even during motion.

In addition to skin-mounted applications, this porous, soft conductor also holds great potential for implantable bioelectronics and soft robots, given its unique properties and capabilities. Overall, the development of this multifunctional porous, soft conductor

represents a significant advancement in the field of bioelectronics, offering promising opportunities for a wide range of biomedical applications.

6 CONCLUSIONS

In conclusion, this engineering thesis has highlighted significant advancements in the field of next-generation skin-interfaced bioelectronics, particularly in the development of elastic soft conductive materials with tissue-like compliance and high stretchability. While various approaches, such as structural designs and intrinsically stretchable materials, have been employed, they often encounter limitations such as rigidity, poor electrical conductivity, and limited stability. Among these approaches, the incorporation of conductive fillers into elastomers, specifically eutectic gallium-indium (EGaIn) nano/microparticles, has shown promise due to their excellent electrical conductivity and fluidity. However, issues related to leaking during deformations have been a challenge.

To address these limitations, this study has presented a phase separation-based synthesis method that creates EGaIn-embedded porous, soft conductors incorporated with epsilon polylysine (ε-PL). This approach offers significant advancements, including high leakage resistance, outstanding antibacterial and antiviral capabilities, and reduced liquid metal usage in elastomer composites. The resulting porous, soft conductors exhibit remarkable properties such as large stretchability, tissue-like compliance, high and stable electrical conductance over deformation, breathability, and compatibility with magnetic resonance imaging (MRI), making them ideal for long-term, stable, and sustainable operation of soft bioelectronics on the skin in daily life scenarios.

Moreover, the application of these porous, soft conductors in skin-interfaced bioelectronics and interconnection cables has been demonstrated, showing their ability to concurrently monitor cardiac electrical and mechanical activities, offer programmed

electrical stimulations, and operate stably and reliably even under dynamic deformations. Importantly, these devices are mechanically imperceptible to users, enhancing their comfort and usability in practical applications. Overall, the findings of this thesis contribute to the advancement of next-generation skin-interfaced bioelectronics, with potential implications in various healthcare and wearable technology applications.

SUPPLIMENTARY FIGURES

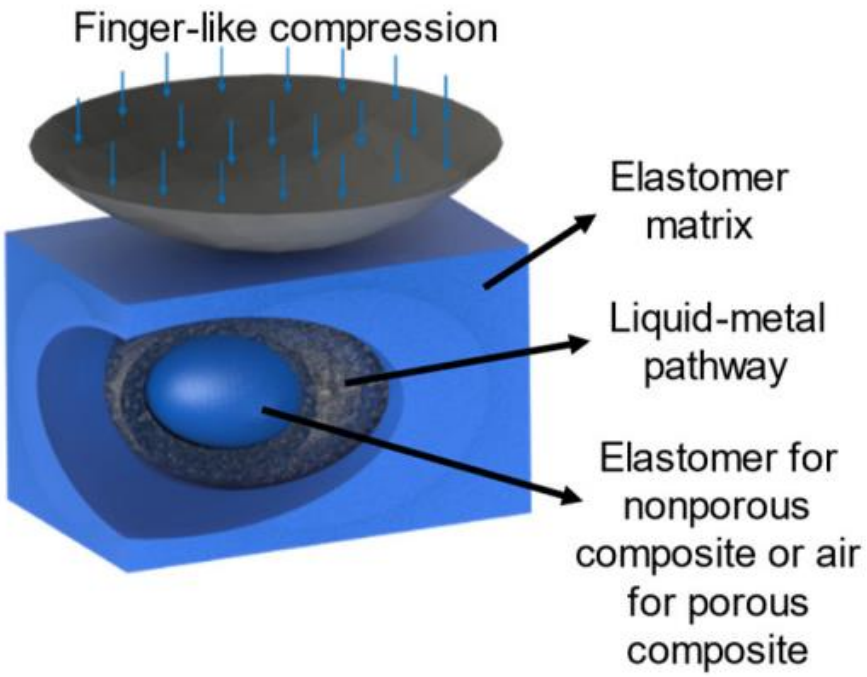

Figure S1: Schematic illustration of the simplified structural model used for FEA Simulations

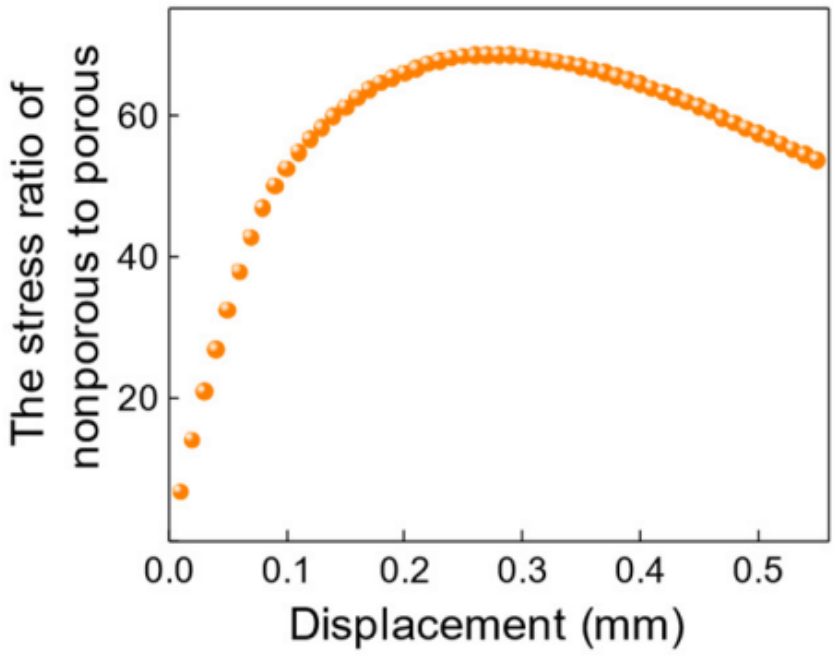

Figure S2: The ratio of the average stress on EGaIn pathways in nonporous and porous composites as a function of the applied displacement

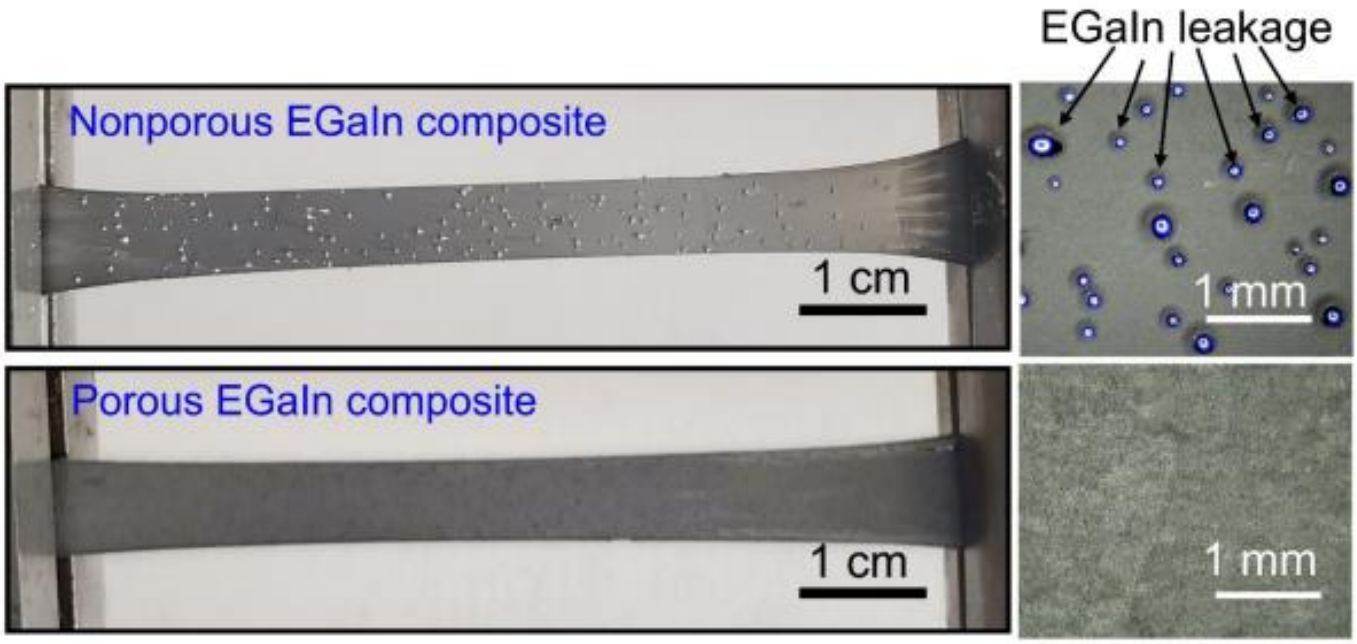

Figure S3: Optical images of cyclic stretching tests (400% strain, 100 cycles) of nonporous and porous EGaIn composites

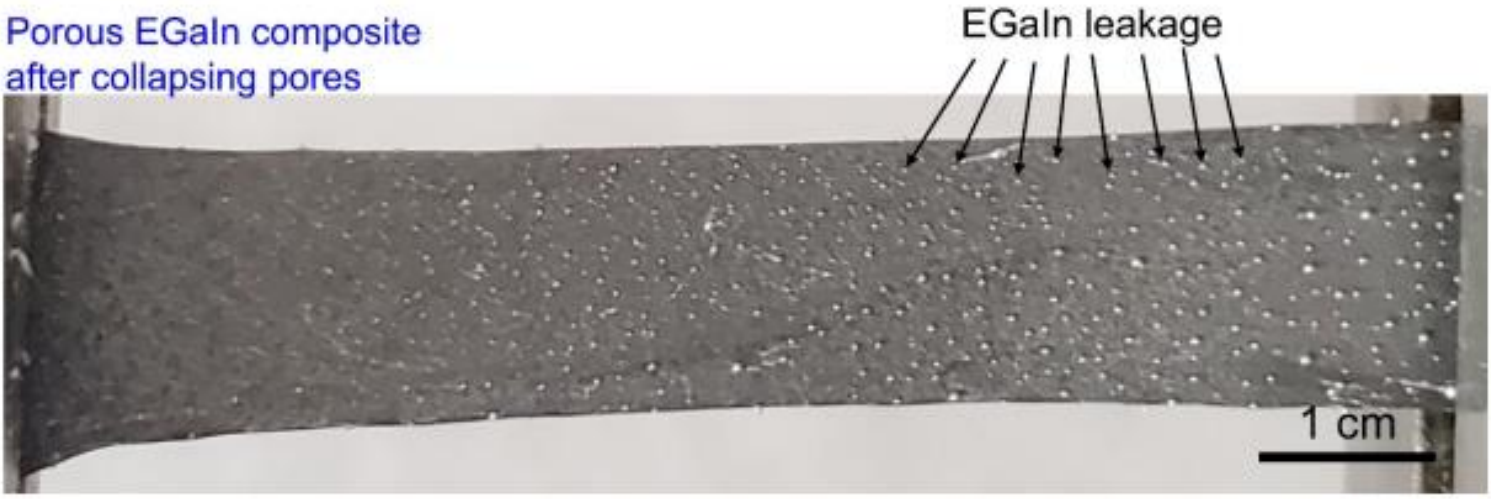

Figure S4: Optical image of the porous EGaIn composite under stretching (300% strain) after its porous structures were collapsed using dimethylformamide vapor

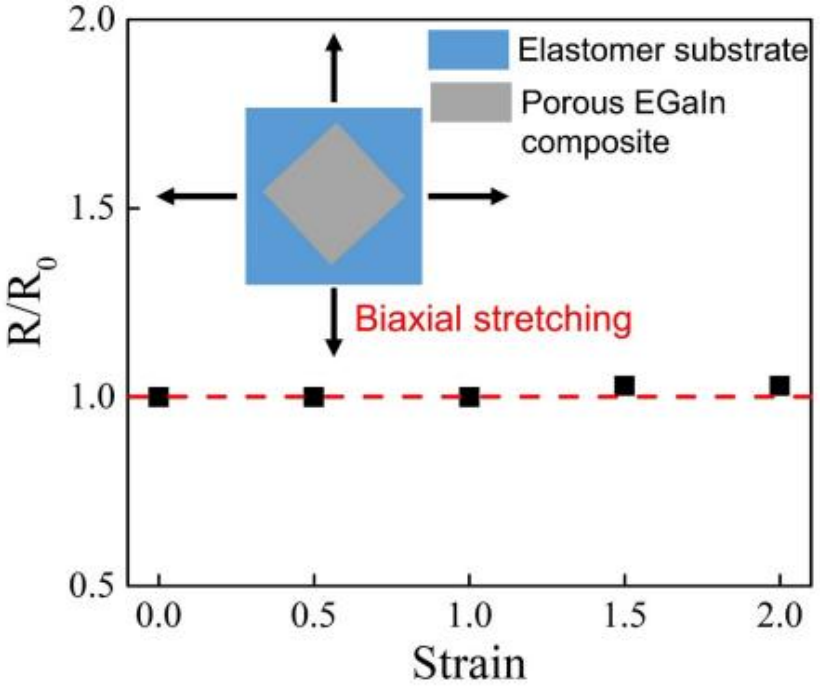

Figure S5:Relative resistance changes (R/R0) of porous EGaIn composites as a function of equally biaxial strains

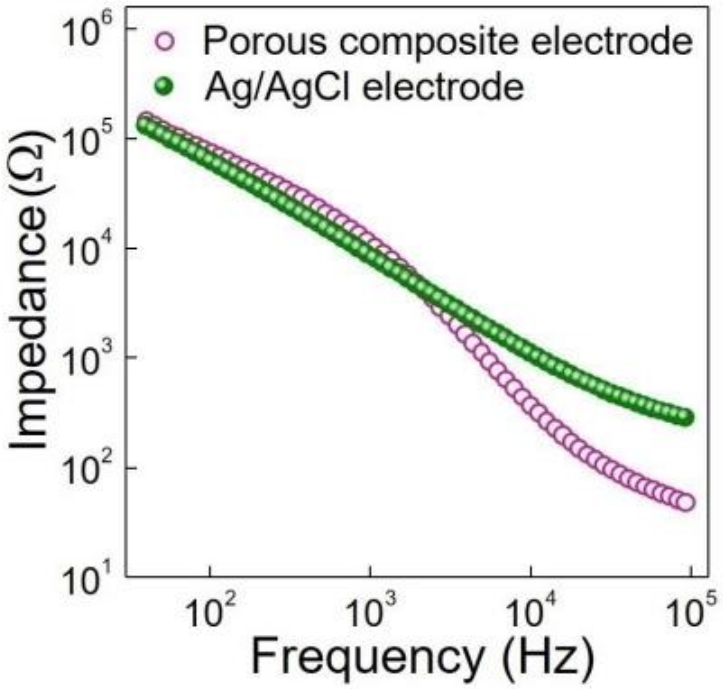

Figure S6: Skin-electrode impedances of porous EGaIn composite electrodes and conventional Ag/AgCl gel electrodes.

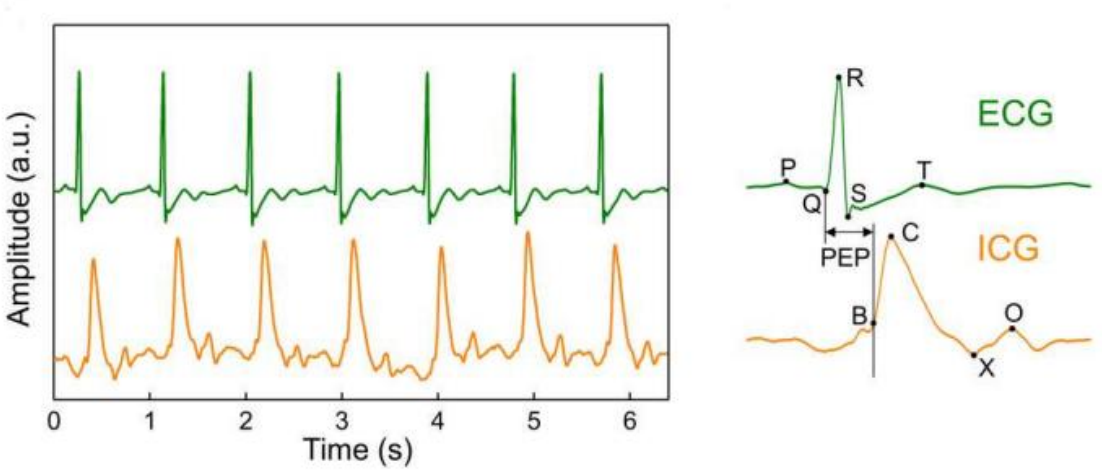

Figure S7: Concurrent ECG and ICG recording using skin-interfaced bioelectronics based on porous EGaIn composites

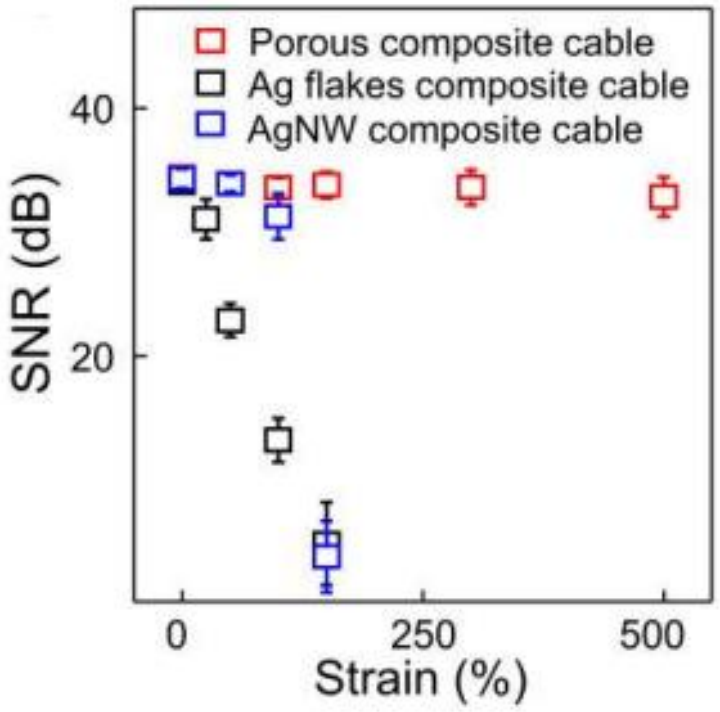

Figure S8: SNR of ECG signals recorded using porous EGaIn composite electrodes when stretching interconnection cables made of porous EGaIn composites, Ag flakes composites, and AgNWs composites

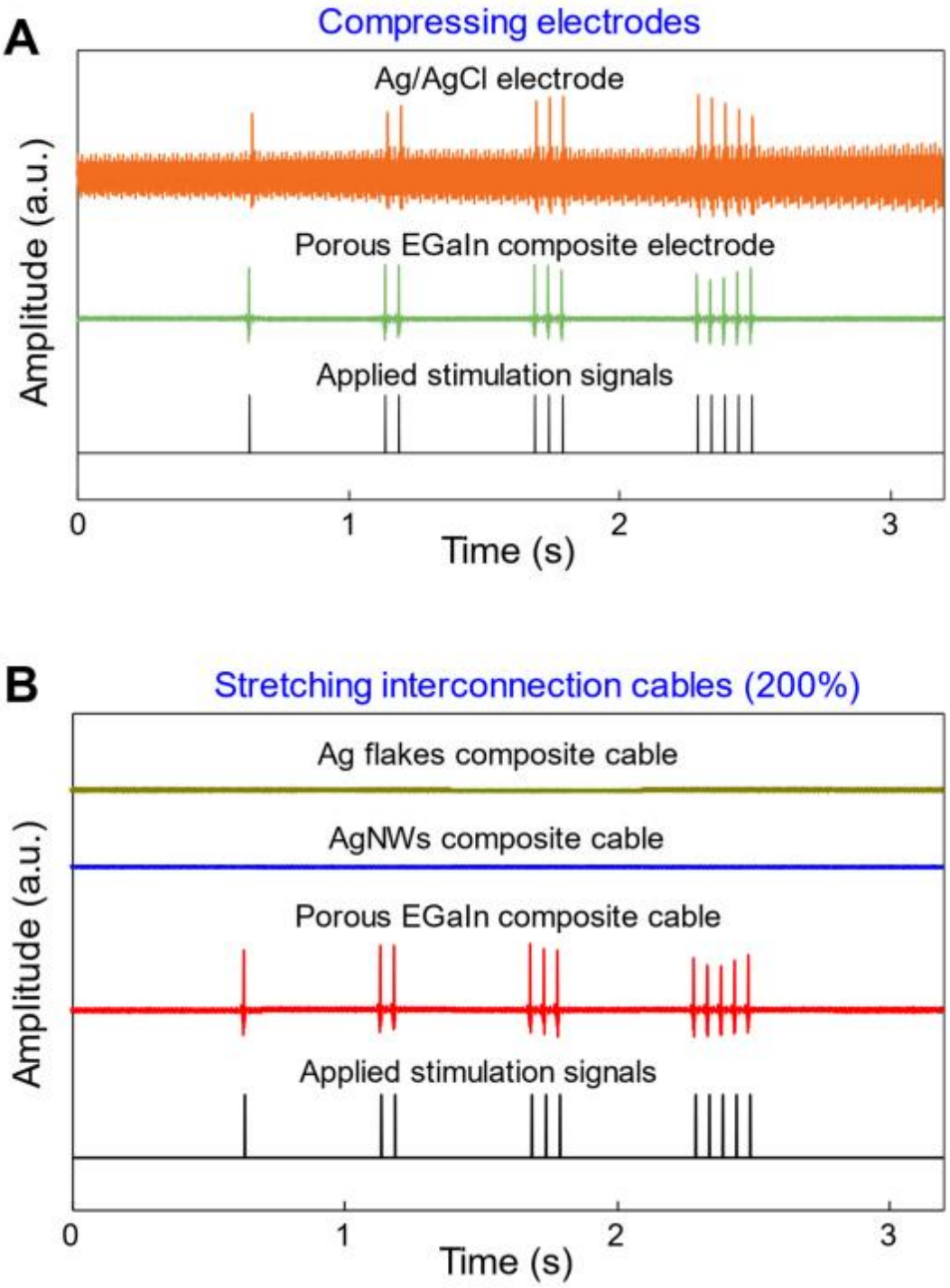

Figure S9: Programmed on-skin electrical stimulations during deformations

REFERENCES

1. J. A. Rogers, T. Someya, Y. Huang, Materials and mechanics for stretchable electronics. Science 327, 1603-1607 (2010).

2. D. H. Kim et al., Epidermal electronics. Science 333, 838-843 (2011).

3. D. C. Kim, H. J. Shim, W. Lee, J. H. Koo, D. H. Kim, Material-based approaches for the fabrication of stretchable electronics. Adv. Mater. 32, 1902743 (2020).

4. K. Sim, Z. Rao, F. Ershad, C. Yu, Rubbery electronics fully made of stretchable elastomeric electronic materials. Adv. Mater. 32, 1902417 (2020).

5. T. C. Shyu et al., A kirigami approach to engineering elasticity in nanocomposites through patterned defects. Nat. Mater. 14, 785-789 (2015).

6. T. Someya, Z. Bao, G. G. Malliaras, The rise of plastic bioelectronics. Nature 540, 379–446 385 (2016).

7. Y. Ohm et al., An electrically conductive silver–polyacrylamide–alginate hydrogel composite for soft electronics. Nat. Electron. 4, 185-192 (2021).

8. K. Sakuma, Flexible, Wearable, and Stretchable Electronics. (CRC Press, 2020).

9. S. Choi et al., Highly conductive, stretchable and biocompatible Ag-Au core-sheath nanowire composite for wearable and implantable bioelectronics. Nat. Nanotechnol. 13, 1048-1056 (2018).

10. Y. Kim et al., Stretchable nanoparticle conductors with self-organized conductive pathways. Nature 500, 59-63 (2013).

11. N. Matsuhisa et al., Printable elastic conductors by in situ formation of silver nanoparticles from silver flakes. Nat. Mater. 16, 834-840 (2017).

12. S. Chen, H.-Z. Wang, R.-Q. Zhao, W. Rao, J. Liu, Liquid metal composites. Matter 2, 1446-1480 (2020).

13. E. J. Markvicka, M. D. Bartlett, X. Huang, C. Majidi, An autonomously electrically self-healing liquid metal–elastomer composite for robust soft-matter robotics and electronics. Nat. Mater. 17, 618-624 (2018).

14. Y. Liu, X. Ji, J. Liang, Rupture stress of liquid metal nanoparticles and their applications in stretchable conductors and dielectrics. npj Flex. Electron. 5, 11 (2021).

15. L. Zheng et al., Conductance-stable liquid metal sheath-core microfibers for stretchy smart fabrics and self-powered sensing. Sci. Adv. 7, eabg4041 (2021).

16. Z. Ma et al., Permeable superelastic liquid-metal fibre mat enables biocompatible and monolithic stretchable electronics. Nat. Mater. 20, 859-868 (2021).

17. S. Xu, A. Jayaraman, J. A. Rogers, Skin sensors are the future of health care. Nature 571, 469 319-321 (2019).

18. R. Ye et al., Antibacterial activity and mechanism of action of ε-poly-l-lysine. Biochem. Biophys. Res. Commun. 439, 148-153 (2013).

19. Y.-Q. Li, Q. Han, J.-L. Feng, W.-L. Tian, H.-Z. Mo, Antibacterial characteristics and mechanisms of ε-poly-lysine against Escherichia coli and Staphylococcus aureus. Food Control 43, 22-27 (2014).

20. M. Hosoya et al., Inhibitory effects of polycations on the replication of enveloped viruses (HIV, HSV, CMV, RSV, influenza A virus and togaviruses) in vitro. Antivir. Chem. Chemother. 2, 243-248 (1991).

21. N. Langeland, L. J. Moore, H. Holmsen, L. Haarr, Interaction of polylysine with the cellular receptor for herpes simplex virus type 1. J. Gen. Virol. 69, 1137-1145 (1988).

22. B. Binks, S. Lumsdon, Pickering emulsions stabilized by monodisperse latex particles: effects of particle size. Langmuir 17, 4540-4547 (2001).

23. K. J. Bretz, Á. Jobbagy, K. Bretz, Force measurement of hand and fingers. Biomech. Hung. 3, 61-66 (2010).

24. M. J. Hessert et al., Foot pressure distribution during walking in young and old adults. BMC Geriatr. 5, 8 (2005).

25. S. Liu, D. S. Shah, R. Kramer-Bottiglio, Highly stretchable multilayer electronic circuits using biphasic gallium-indium. Nat. Mater. 20, 851-858 (2021).

26. M. H. Malakooti et al., Liquid metal supercooling for low-temperature thermoelectric wearables. Adv. Funct. Mater. 29, 1906098 (2019).

27. T. Someya, M. Amagai, Toward a new generation of smart skins. Nat. Biotechnol. 37, 382-388 (2019).

28. S. Chao et al., Synthesis and characterization of tigecycline-loaded sericin/poly (vinyl alcohol) composite fibers via electrospinning as antibacterial wound dressings. J. Drug Deliv. Sci. Technol. 44, 440-447 (2018).

29. X. Zheng et al., Ultralight, ultrastiff mechanical metamaterials. Science 344, 1373-1377 (2014).

30. S. Liu, Y. Rao, H. Jang, P. Tan, N. Lu, Strategies for body-conformable electronics. Matter 5, 1104-1136 (2022).

31. L. Tian et al., Large-area MRI-compatible epidermal electronic interfaces for prosthetic control and cognitive monitoring. Nat. Biomed. Eng. 3, 194 (2019).

32. N. Driscoll et al., MXene-infused bioelectronic interfaces for multiscale electrophysiology and stimulation. Sci. Transl. Med. 13, eabf8629 (2021).

33. J. F. Schenck, The role of magnetic susceptibility in magnetic resonance imaging: MRI magnetic compatibility of the first and second kinds. Med. Phys. 23, 815-850 (1996).

34. Y. Xie et al., Motion robust ICG measurements using a two-step spectrum denoising method. Physiol. Meas. 42, 095004 (2021).

35. K. Ushimaru, Y. Hamano, H. Katano, Antimicrobial activity of ε-poly-L-lysine after forming a water-insoluble complex with an anionic surfactant. Biomacromolecules 18, 1387-1392 (2017).

36. H.-W. Zhu et al., Printable elastic silver nanowire-based conductor for washable electronic textiles. Nano Res. 13, 2879-2884 (2020).

37. Y. Khan et al., Design considerations of a wearable electronic-skin for mental health and wellness: balancing biosignals and human factors. bioRxiv, (2021).

38. N. Cohen, K. Bhattacharya, A numerical study of the electromechanical response of liquid metal embedded elastomers. Int. J. Non-Linear Mech. 108, 81-86 (2019).

39. M. Geerligs et al., In vitro indentation to determine the mechanical properties of epidermis. J. Biomech. 44, 1176-1181 (2011).

40. M. L. Crichton et al., The viscoelastic, hyperelastic and scale dependent behaviour of freshly excised individual skin layers. Biomaterials 32, 4670-4681 (2011).

41. Y. Xu et al., Porous liquid metal–elastomer composites with high leakage resistance and antimicrobial property for skininterfaced bioelectronics. Science Advances, (2023).

42. S. Mansouri, T. Alhadidi, S. Chabchoub, R. B. Salah, Impedance cardiography: Recent applications and developments. Biomed. Res. 29, 3542–3552 (2018).

43. D. Naranjo-Hernández, J. Reina-Tosina, M. Min, Fundamentals, recent advances, and future challenges in bioimpedance devices for healthcare applications. J. Sens. 2019, 9210258 (2019).

44. Y. Xie, R. Song, D. Yang, H. Yu, C. Sun, Q. Xie, R. X. Xu, Motion robust ICG measurements using a two-step spectrum denoising method. Physiol. Meas. 42, 095004 (2021).